

Assessment of cerebral microbleeds by susceptibility-weighted imaging at 3T in patients with end-stage organ failure

Gianvincenzo Sparacia, Roberto Cannella, Vincenzina Lo Re, Angelo Gambino, Giuseppe Mamone & Roberto Miraglia

La radiologia medica

Official Journal of the Italian Society of Medical Radiology

ISSN 0033-8362

Radiol med

DOI 10.1007/s11547-018-0863-x



Your article is protected by copyright and all rights are held exclusively by Italian Society of Medical Radiology. This e-offprint is for personal use only and shall not be self-archived in electronic repositories. If you wish to self-archive your article, please use the accepted manuscript version for posting on your own website. You may further deposit the accepted manuscript version in any repository, provided it is only made publicly available 12 months after official publication or later and provided acknowledgement is given to the original source of publication and a link is inserted to the published article on Springer's website. The link must be accompanied by the following text: "The final publication is available at link.springer.com".



Assessment of cerebral microbleeds by susceptibility-weighted imaging at 3T in patients with end-stage organ failure

Gianvincenzo Sparacia^{1,2} · Roberto Cannella¹ · Vincenzina Lo Re³ · Angelo Gambino¹ · Giuseppe Mamone² · Roberto Miraglia²

Received: 14 October 2017 / Accepted: 7 February 2018
© Italian Society of Medical Radiology 2018

Abstract

Purpose Cerebral microbleeds (CMBs) are small rounded lesions representing cerebral hemosiderin deposits surrounded by macrophages that results from previous microhemorrhages. The aim of this study was to review the distribution of cerebral microbleeds in patients with end-stage organ failure and their association with specific end-stage organ failure risk factors.

Materials and methods Between August 2015 and June 2017, we evaluated 15 patients, 9 males, and 6 females, (mean age 65.5 years). Patients population was subdivided into three groups according to the organ failure: (a) chronic kidney failure ($n = 8$), (b) restrictive cardiomyopathy undergoing heart transplantation ($n = 1$), and (c) end-stage liver failure undergoing liver transplantation ($n = 6$). The MR exams were performed on a 3T MR unit and the SWI sequence was used for the detection of CMBs. CMBs were subdivided in supratentorial lobar distributed, supratentorial non-lobar distributed, and infratentorial distributed.

Results A total of 91 microbleeds were observed in 15 patients. Fifty-nine CMBs lesions (64.8%) had supratentorial lobar distribution, 17 CMBs lesions (18.8%) had supratentorial non-lobar distribution and the remaining 15 CMBs lesions (16.4%) were infratentorial distributed. An overall predominance of supratentorial multiple lobar localizations was found in all types of end-stage organ failure. The presence of CMBs was significantly correlated with age, hypertension, and specific end-stage organ failure risk factors ($p < 0.001$).

Conclusions CMBs are mostly founded in supratentorial lobar localization in end-stage organ failure. The improved detection of CMBs with SWI sequences may contribute to a more accurate identification of patients with cerebral risk factors to prevent complications during or after the organ transplantation.

Keywords Cerebral microbleeds · Susceptibility-weighted imaging · Magnetic resonance imaging · End-stage organ failure · Transplantation

Introduction

Cerebral microbleeds (CMBs) consist of small cerebral hemosiderin deposits surrounded by macrophages that result from previous microhemorrhages, usually asymptomatic due to the rupture of small arteries, arterioles, and/or capillaries [1, 2]. Cerebral microbleeds can be visualized on T2*-weighted gradient-recalled-echo (GRE) magnetic resonance (MR) imaging sequences, as small, rounded, or ovoid blooming homogeneous hypointense lesions, localized in the brain parenchyma, measuring 5–10 mm in diameter [3–6].

In recent years, the introduction of susceptibility-weighted imaging (SWI) MR sequences has improved CMBs detection of previously undetected small intracerebral

✉ Gianvincenzo Sparacia
gsparacia@ismett.edu

¹ Department of Radiology, University of Palermo, Palermo, Italy

² Department of Diagnostic and Therapeutic Services, IRCCS-ISMETT (Mediterranean Institute for Transplantation and Advanced Specialized Therapies), Palermo, Italy

³ Neurology Unit, IRCCS-ISMETT (Mediterranean Institute for Transplantation and Advanced Specialized Therapies), Palermo, Italy

hemorrhages (< 5–10 mm in diameter) compared to the GRE MR sequences [7, 8].

The SWI sequence is a velocity compensated high-resolution 3D gradient-echo sequence that uses magnitude and filtered phase information to create a new contrast [9, 10]. As a result, CMBs are more sensitively detected by SWI compared to T2*-weighted GRE [3, 8, 11–14].

The presence of cerebral microbleeds was found in up to 5% of healthy adults, but they were most commonly correlated with aging, hypertension, cerebral amyloid angiopathy, ischemic stroke, intracerebral hemorrhage, and cognitive disorders [1, 12, 15]. In these patients, CMBs represent an important marker of the cerebral small vessel pathology [7, 16, 17]. Moreover, the presence of CMBs is an independent risk factor for subsequent larger intracerebral hemorrhages, and they are also associated with higher incidence of cognitive decline [18, 19].

Regarding the localization, cerebral microbleeds can be classified in supratentorial lobar, supratentorial deep (or non-lobar), infratentorial, and mixed distributed.

The lobar distribution involves the cortex and the subcortical white matter. Deep CMBs are localized in the basal ganglia, internal and external capsule, thalamus, deep and periventricular white matter. The infratentorial pattern includes the brainstem and cerebellum. Finally, mixed CMBs are a combination of both cortical and deep localization [20].

The distribution of CMBs could be correlated to the systemic disease of the patient.

A supratentorial lobar pattern was associated with the presence of cerebral amyloid angiopathy [21] and with degenerative brain disease, most commonly Alzheimer disease [11, 22, 23]. A distribution of CMBs in the deep white matter or in the infratentorial structure was significantly higher in patients with hypertension [16].

Patients with end-stage organ failure share several risk factors strongly associated with the presence of cerebral microbleeds, such as cardiovascular risk factors, low glomerular filtration rate, and platelet dysfunction. Moreover, advanced hepatic failure, such as in Child–Pugh class C, or fulminant hepatitis, are associated with hepatic coagulopathy due to decreased liver production of coagulation proteins [24].

Cerebral microbleeds have also an increased incidence in patients who underwent anticoagulation therapy due to chronic heart disease that finally brings to end-stage heart failure [25].

As the presence of CMBs is considered a risk factor for future development of CMBs, and it may predict the development of ischaemic stroke and secondary intracranial hemorrhage [26, 27], it has become of fundamental relevance to assess the number and distribution of CMBs by MR imaging [3–6].

The aim of this study was to review the distribution of cerebral microbleeds in patients with end-stage organ failure and their association with specific end-stage organ failure risk factors as a neuroimaging biomarker for the underlying disease.

Materials and methods

Patient population

Our retrospective cohort study was reviewed and approved by the Institutional Research Review Board (IRRB) of our institution, and informed consent form was waived; however, informed written consent to the MR was obtained in all patients.

We examined 79 patients candidate for liver, kidney or heart transplantation between August 2015 and June 2017 as a part of a research protocol aimed to assess preexistence of cerebral risk factor in patients candidate for organ transplantation at our institution. Among the 79 patients, only 29 consecutive patients who underwent brain MR imaging at 3T were selected while the remaining 50 patients that underwent brain MR imaging at 1.5T were excluded.

Patients were referred for end-stage liver, kidney or heart failure, according to following clinical characteristics: stage 5 chronic kidney failure having estimated glomerular filtration rate (eGFR) less than 15, or patient already on dialysis; chronic heart failure classified with the New York Heart Association (NYHA) criteria [28] on class III or IV, requiring heart transplantation; end-stage hepatic failure due to cirrhosis requiring hepatic transplantation in Child–Pugh class B–C [24].

Clinical and laboratory data were collected for each patient including duration of the disease leading to end-stage organ failure, hypertension, diabetes mellitus, hyperlipidemia, coronary artery disease, atrial fibrillation, glomerular filtration rate, platelet dysfunction, and hepatic coagulopathy. Drug therapy, which could increase bleeding risk, such as aspirin, clopidogrel, and warfarin, was reported for each patient.

Exclusion criteria were the presence of acute or chronic ischemic or hemorrhagic stroke, intracranial hemangioma, cerebral cavernous malformation, arteriovenous malformations, cerebral aneurysm, Alzheimer's disease, intracerebral lesions with a hemorrhagic component associated with tumors and abscesses.

Patients with unavailable SWI images ($n = 8$), or poor image quality ($n = 6$) were excluded from the study.

Ultimately, the study population consisted of 15 patients (mean age 63.5 years, age range 48–82 years, ± 9.15), 9 males (60%) and 6 females (40%).

Patients population was subdivided into three groups according to the organ failure: patients with end-stage kidney failure ($n = 8$), a patient undergoing heart transplantation due to restrictive cardiomyopathy ($n = 1$), and patients with end-stage liver failure undergoing liver transplantation ($n = 6$). Data are summarized in Table 1.

MR examination

The MR exams were performed on a 3T MR scanner (Discovery 750w, General Electric, Healthcare, Milwaukee, USA).

MR imaging protocol included axial and sagittal fast-spin echo (FSE) T2W (8000/90 [TR/TE]) images, axial fluid-attenuated inversion-recovery (FLAIR) (9000/150/2250 [TR/TE/TI]) images, along with axial, sagittal and coronal non-enhanced and contrast-enhanced (0.1 mmol/kg gadobutrol–Gadovist, Bayer, Germany), FSE T1W (600/20 [TR/TE]) images with a field of view (FOV) of 24 cm, matrix 320×320 , slice thickness 4 mm, intersection gap 1 mm, number of excitations 1.

The SWI images (3D GRE 48/23 ms [TR/TE], flip angle 10°) were obtained with a FOV of 24 cm, matrix 256×256 , slice thickness 2.5 mm, gap 1 mm, number of excitations 1, and acquisition time 4:04 min.

The SWI images were also post-processed with the minimum intensity projection (MinIP) algorithm in the axial plane with a slice thickness of 3–10 mm to better visualize “signal void” of the vessels structures.

Image analysis

The images were analyzed in consensus by two neuroradiologists, each with at least 10 years of experience, who were unaware of the patients' clinical information. Any disagreement about image assessment was resolved in consensus by the two radiologists by discussion.

SWI images, presented in random order on a picture archiving and communication system (PACS) (Agfa Health-Care GmbH—Bonn, Germany), were analyzed by the two neuroradiologists for the presence and localization of the CMBs lesions.

Table 1 Characteristics of patients

Variables	No.
Number of patients	15
Mean age (\pm SD), years	63.5 (\pm 9.15)
Sex (male/female)	9/6
End-stage kidney failure	8
End-stage heart failure	1
End-stage liver failure	6

Cerebral microbleeds were defined as small, hypointense, rounded lesions within the brain parenchyma that measured less than 10 mm on the SWI images [29].

Using the SWI-filtered phase images, cortical calcifications, as well as choroid plexus, globus pallidum, and pineal calcifications, were easily identified as they appear with the opposite-sign phase compared to hemosiderin [30]. Hypointense lesions in the basal ganglia, not clearly identified as calcifications, were excluded as most likely they represent iron deposits.

Hypointense spots near the neurocranium and the splanchnocranium were not considered because of their vicinity to the bone and their consequent uncertain artifact nature.

To better differentiate between CMBs and blood vessels, the minimum intensity projection (MinIP) post-processed SWI images were used as they are able to demonstrate the “signal void” of the vessels structures [5].

Number and distribution of cerebral microbleeds were recorded based on their location as supratentorial lobar (strictly cortical and subcortical), supratentorial non-lobar (in deep regions including the basal ganglia, thalamus, internal capsule, external capsule, corpus callosum, deep and periventricular white matter), and infratentorial (brainstem, cerebellum) as previously reported in the literature [29].

Statistical analysis

Continuous variables are presented as mean \pm standard deviation (SD) and compared using two-tailed, unpaired Student's *t* test. Fisher's test was used to test for differences in categorical variables.

Multivariate logistic regression analysis was performed to assess the association between the number of CMBs lesions with patient's age, sex, duration of the disease leading to end-stage organ failure, hypertension, diabetes mellitus, and hyperlipidemia.

Multivariate regression analysis was then performed taking in account risk factors specific for end-stage liver, kidney, or heart failure such as platelet dysfunction and hepatic coagulopathy, glomerular filtration rate, coronary artery disease, atrial fibrillation, and drug therapy which could increase bleeding risk.

Differences for a *p* value of < 0.05 were considered statistically significant.

Statistical analysis was performed using the statistical software package SPSS (SPSS, Chicago, USA).

Results

Cerebral microbleeds were demonstrated as small, rounded, hypointense lesions within the brain parenchyma that measured less than 10 mm on the SWI images.

A total of 91 microbleeds were observed in 15 patients. Fifty-nine CMBs lesions (64.8%) had supratentorial lobar distribution, 17 CMBs lesions (18.8%) had supratentorial non-lobar distribution, and the remaining 15 CMBs lesions (16.4%) were infratentorial distributed (Figs. 1, 2, 3, 4) (Table 2).

The mean count of microbleeds was $3.9 (\pm 5.4)$ per patient for supratentorial lobar distribution, $1.1 (\pm 1.1)$ per patient for supratentorial non-lobar distribution, and $1 (\pm 1.4)$ per patient for infratentorial distribution.

The frequency of the number of CMBs was as follow: three patients (3%) had one microbleed, ten patients (50.8%) had multiple microbleeds ranging from 2 to 9 microbleeds, one patient (17.6%) had 16 microbleeds and one patient (28.6%) had 26 microbleeds.

A predominance of supratentorial lobar distribution of CMBs was seen in all type of end-stage organ failure, and it was characterized by the presence of multiple CMBs (range 2–26 CMBs) (Table 2).

The number of CMBs were significantly correlated with the age of the patients (age coefficient 0.56, $p < 0.001$), which means that the older the patients the more numerous the CMBs were found.

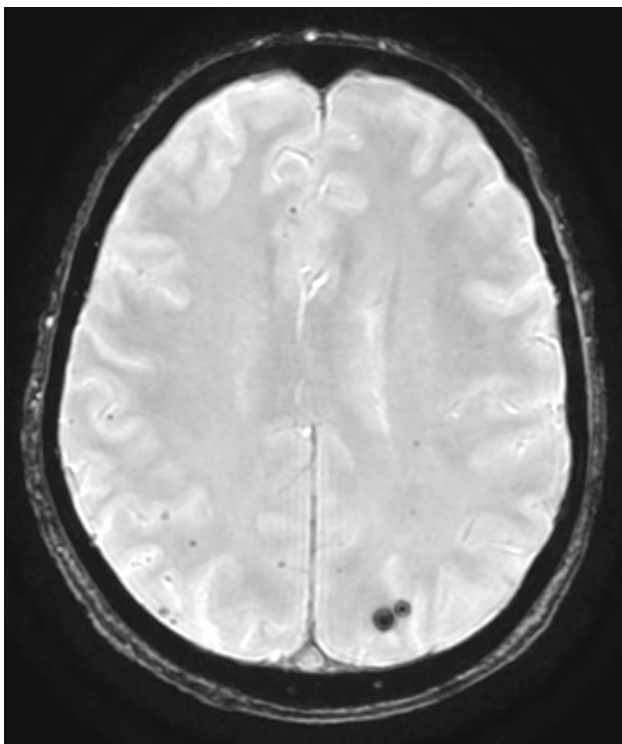


Fig. 1 Supratentorial lobar distributed cerebral microbleeds in end-stage kidney failure patient. Axial minimum intensity projection (MinIP) susceptibility-weighted imaging (SWI) image shows two small, rounded, hypointense cerebral microbleeds in the left parietal lobe, and other smaller microbleeds in both frontal and parietal lobes of the right and left hemispheres

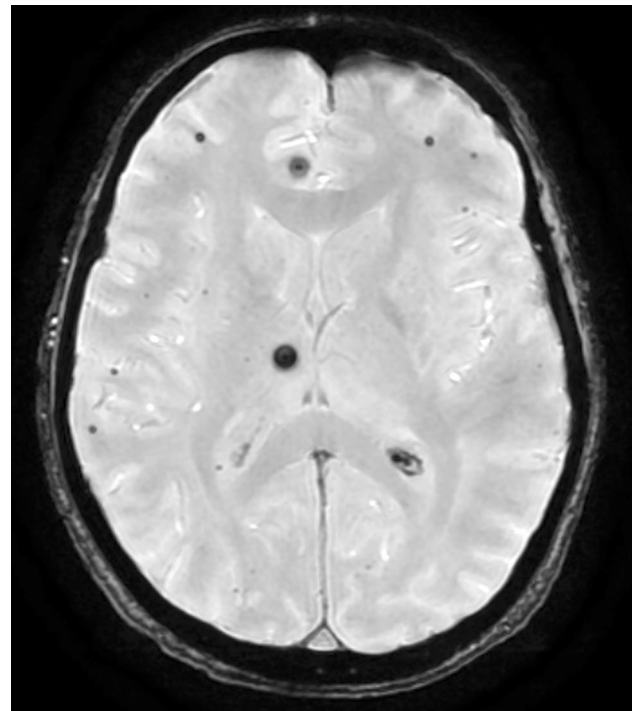


Fig. 2 Supratentorial lobar and non-lobar distributed cerebral microbleeds in end-stage hepatic failure patient. Axial minimum intensity projection (MinIP) susceptibility-weighted imaging (SWI) image shows a rounded, hypointense, non-lobar cerebral microbleed in the right thalamus, and several small rounded, hypointense, lobar distributed cerebral microbleeds in the left and right frontal lobes, and in the right temporal and parietal gray/white matter junction

In multivariate logistic regression analysis, adjusted for age and sex, the presence of CMBs was significantly correlated with hypertension ($p = 0.001$), diabetes ($p = 0.015$), duration of the disease leading to end-stage organ failure ($p = 0.002$), glomerular filtration rate ($p = 0.001$), platelet dysfunction ($p = 0.008$), hepatic coagulopathy ($p = 0.006$), and anticoagulation or antiplatelet drug therapy ($p = 0.001$).

Discussion

The results of our study show that the presence of cerebral microbleeds is significantly correlated with several risk factors related to end-stage liver, kidney or heart failure such as low glomerular filtration rate, platelet dysfunction, hepatic coagulopathy, anticoagulation or antiplatelet drug therapy, and duration of the disease leading to end-stage organ failure. Age and hypertension are also significantly correlated to the presence of CMBs as demonstrated in this study and as reported in the literature [19].

Cerebral microbleeds, according to guideline proposed in the literature [3–6], are defined as round or ovoid lesions, that appear hypointense and with a blooming effect

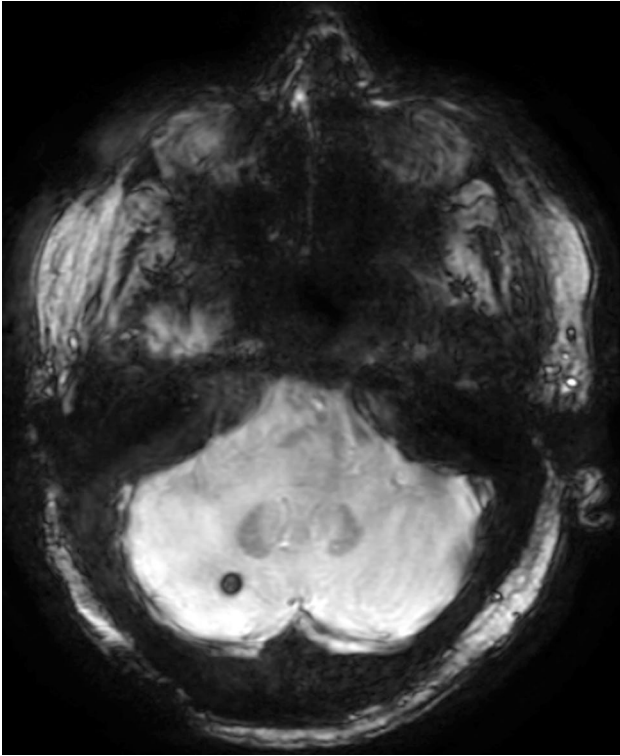


Fig. 3 Infratentorial distributed cerebral microbleed in end-stage heart disease patient. Axial minimum intensity projection (MinIP) susceptibility-weighted imaging (SWI) image shows a small, rounded, hypointense, right cerebellar hemisphere microbleed

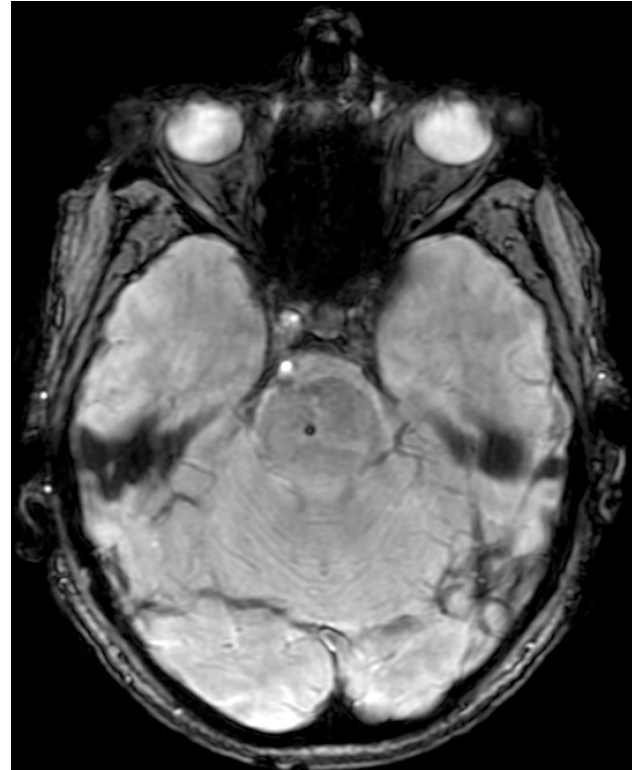


Fig. 4 Infratentorial distributed cerebral microbleed in end-stage heart disease patient. Axial minimum intensity projection (MinIP) susceptibility-weighted imaging (SWI) image shows a small, rounded, hypointense, brainstem microbleed

on T2*-GRE and SWI sequences. CMBs represent small perivascular hemosiderin deposits surrounded by normal brain tissue. After extravasation of erythrocytes into the perivascular space, degradation of hemoglobin contained in the erythrocytes leads to the formation of hemosiderin. Hemosiderin is a paramagnetic substance which can be detected by T2*-GRE and SWI MR sequences [19].

The detection of CMBs depends on many MR imaging parameters, such as field strength, echo time, and resolution. In recent years, with the introduction of susceptibility-weighted imaging sequences, and with the wider availability of 3T MR units, there was an increased sensitivity of detection of small cerebral microbleeds [7, 8, 19].

Supratentorial lobar distribution of cerebral microbleeds was the most typical distribution founded in our series of end-stage organ failure patients (64.8%), and it was characterized by the presence of multiple cortical and subcortical white matter CMBs (range 2–26 CMBs). Particularly, the highest number ($n = 45$) of lobar CMBs was seen in patients with chronic kidney failure.

A lobar distribution of CMBs is considered to relate to cerebral amyloid angiopathy, while CMBs located in the basal ganglia or in infratentorial brain regions are thought to relate to hypertensive vasculopathy [21].

Table 2 Distribution of cerebral microbleeds (CMBs)

Location	CMBs (n)	%
Supratentorial lobar	59	64.8
Supratentorial non-lobar	17	18.7
Infratentorial	15	16.5
Total	91	100

Location: *Lobar* supratentorial CMBs located in cortical-subcortical parenchyma of frontal, parietal, occipital or temporal lobes, *Non-lobar* supratentorial CMBs located in supratentorial deep regions including the basal ganglia, thalamus, internal capsule, external capsule, corpus callosum, deep and periventricular white matter, *Infratentorial* CMBs located in brainstem and cerebellum

CMBs cerebral microbleeds

Our results confirm that cerebral microbleeds can be commonly found in patients with chronic kidney failure, especially in dialytic patients [31]. This association was not related to the presence of other CMB risk factors such as other neurological diseases [32].

The incidence of microbleeds in hemodialysis patients is significantly higher compared with the general population without a history of chronic kidney failure or stroke.

In the chronic kidney failure population, diminished estimated glomerular filtration rate has been found to be a risk factor for CMBs [31]. Moreover, chronic kidney failure is correlated with the number of CMBs, thus, the number of CMBs can provide an indirect estimation of chronic kidney failure severity [33–36].

In our patient who underwent heart transplantation, a predominance of supratentorial lobar distribution of CMBs was found. The anticoagulant therapy, in this case, was the major risk factor that explains the presence of cerebral microbleeds. Although it has been established that warfarin treatment is effective for preventing cerebral embolism arising from atrial fibrillation, the most serious adverse event in atrial fibrillation is hemorrhage complication [25].

The literature evidence suggests that the presence of cerebral microbleeds is a risk factor for intracerebral hemorrhage in patients treated with antiplatelet therapy and a higher risk of mortality was demonstrated for patients with more than five cerebral microbleeds [37].

Ueno et al. [27] demonstrated how the presence of cerebral microbleeds may be an independent risk factor for warfarin-related intracerebral hemorrhage. Also, Lee et al. [38] found that the presence of cerebral microbleeds was more commonly found in patients with warfarin-related intracerebral hemorrhage when compared to anticoagulated patients without intracerebral hemorrhage.

In end-stage liver failure patients studied in our series, the most common complication of the disease was the hepatic encephalopathy, which is an important prognostic factor of the disease [39].

Hepatic encephalopathy is characterized by high signal intensity in the globus pallidum on T1-weighted MR images, likely a reflection of increased tissue concentrations of manganese, and white matter abnormality [40].

However, hepatic failure is also associated with coagulopathy due to decreased liver production of coagulation proteins. The presence of CMBs on SWI images was reported in patients with hepatic coagulopathy in the corpus callosum and in the paraventricular white matter, and they may arise from rupture of small penetrating arterial vessels [41].

Cerebral microbleeds were related to the degree of liver fibrosis, with a significantly increased number of cerebral microhemorrhages in case of advanced fibrosis [42].

In our series, supratentorial lobar distribution of CMBs was the most commonly reported location in end-stage liver disease patients with a significant positive correlation with platelet dysfunction and hepatic coagulopathy due to decreased liver production of coagulation proteins in advanced hepatic failure.

There is clinical evidence for the role of cerebral microbleeds in cognitive decline and for the correlation between CMBs and small vessel disease, cerebral stroke, and increase mortality. Particularly, there is strong evidence that higher

number of CMBs is associated with a more severe cognitive dysfunction, which comprises impaired executive function, and decreased attention and processing speed [7, 11, 34]. The development of novel imaging technique and large prospective studies is expected to better understand the pathogenesis of CMBs and the clinical implication of this currently underdiagnosed clinical entity.

Limitations of this study are the relatively small group of patients, the lack of randomization of groups, the prevalence of end-stage kidney failure patients over other end-stage organ failure, particularly to the only one end-stage heart failure patient, and the retrospective nature of the study.

Another limitation was due to the fact that patient image analysis was limited by the lack of SWI images ($n = 8$) or poor image quality ($n = 6$) due to the motion artifact.

Conclusions

The use of SWI sequences in a more widely available very high field strength MR units (3T) has increased the detection of CMBs underlying an emerged new important imaging biomarker of cerebral involvement in a variety of diseases and syndromes.

Cerebral microbleeds are mostly founded in supratentorial lobar localization in end-stage organ failure patients and they are associated to several specific risk factors related to end-stage organ failure.

The radiologist involved in brain imaging in end-stage organ failure patients should be aware of the evidence that the presence of CMBs might identify patients at risk of future cerebral stroke, intracranial hemorrhage, and cognitive impairment, which in turn represents risk factor for complication during or after the transplantation.

Funding The authors state that this work has not received any funding.

Compliance with ethical standards

Conflict of interest The scientific guarantor of this publication is Gianvincenzo Sparacia, MD. The authors of this manuscript declare no relationships with any companies, whose products or services may be related to the subject matter of the article.

Ethical standards Our retrospective cohort study was reviewed and approved by the Institutional Research Review Board (IRRB) of our institution, and informed consent form was waived.

Informed consent Written informed consent to the MR exam was obtained from all subjects (human participants, patients) in this study.

References

1. Yates PA, Villemagne VL, Ellis KA, Desmond PM, Masters CL, Rowe CC (2014) Cerebral microbleeds: a review of clinical, genetic, and neuroimaging associations. *Front Neurol* 6(4):205
2. Linn J (2015) Imaging of cerebral microbleeds. *Clin Neuroradiol* 25(Suppl 2):167–175
3. Nandigam RN, Viswanathan A, Delgado P, Skehan ME, Smith EE, Rosand J, Greenberg SM, Dickerson BC (2009) MR imaging detection of cerebral microbleeds: effect of susceptibility-weighted imaging, section thickness, and field strength. *AJNR Am J Neuroradiol* 30:338–343
4. Fazekas F, Kleinert R, Roob G, Kleinert G, Kapeller P, Schmidt R, Hartung HP (1999) Histopathologic analysis of foci of signal loss on gradient-echo T2*-weighted MR images in patients with spontaneous intracerebral hemorrhage: evidence of microangiopathy-related microbleeds. *AJNR Am J Neuroradiol* 20:637–642
5. Charidimou A, Krishnan A, Werring DJ, Jäger HR (2013) Cerebral microbleeds: a guide to detection and clinical relevance in different disease settings. *Neuroradiology* 55(6):655–674
6. Greenberg SM, Vernooij MW, Cordonnier C, Viswanathan A, Salman RA, Warach S, Launer LJ, Van Buchem MA, Breteler MM, Microbleed Study Group (2009) Cerebral microbleeds: a guide to detection and interpretation. *Lancet Neurol* 8:165–174
7. Zhou H, Yang J, Xie P, Dong Y, You Y, Liu J (2017) Cerebral microbleeds, cognitive impairment, and MRI in patients with diabetes mellitus. *Clin Chim Acta* 470:14–19
8. Sparacia G, Speciale C, Banco A, Bencivinni F, Midiri M (2016) Accuracy of SWI sequences compared to T2*-weighted gradient echo sequences in the detection of cerebral cavernous malformations in the familial form. *Neuroradiol J* 29:326–335
9. Haacke EM, Mittal S, Wu Z, Neelavalli J, Cheng YC (2009) Susceptibility-weighted imaging: technical aspects and clinical applications, part 1. *AJNR Am J Neuroradiol* 30:19–30
10. Mittal S, Wu Z, Neelavalli J, Haacke EM (2009) Susceptibility-weighted imaging: technical aspects and clinical applications, part 2. *AJNR Am J Neuroradiol* 30:232–252
11. Sparacia G, Agnello F, La Tona G, Iaia A, Midiri F, Sparacia B (2017) Assessment of cerebral microbleeds by susceptibility-weighted imaging in Alzheimer's disease patients: a neuroimaging biomarker of the disease. *Neuroradiol J* 30:330–335
12. Goos JD, van der Flier WM, Knol DL, Pouwels PJ, Scheltens P, Barkhof F, Wattjes MP (2011) Clinical relevance of improved microbleed detection by susceptibility-weighted magnetic resonance imaging. *Stroke* 42:1894–1900
13. Mori N, Miki Y, Kikuta K, Fushimi Y, Okada T, Urayama S, Sawamoto N, Fukuyama H, Hashimoto N, Togashi K (2008) Microbleeds in moyamoya disease: susceptibility-weighted imaging versus T2*-weighted imaging at 3 Tesla. *Invest Radiol* 43:574–579
14. Guo LF, Wang G, Zhu XY, Liu C, Cui L (2013) Comparison of ESWAN, SWI-SPGR, and 2D T2*-weighted GRE sequence for depicting cerebral microbleeds. *Clin Neuroradiol* 23:121–127
15. Shams S, Granberg T, Martola J, Charidimou A, Li X, Shams M, Fereshtehnejad SM, Cavallin L, Aspelin P, Wiberg-Kristoffersen M, Wahlund LO (2017) Cerebral microbleeds topography and cerebrospinal fluid biomarkers in cognitive impairment. *J Cereb Blood Flow Metab* 37:1006–1013
16. Yakushiji Y (2015) Cerebral microbleeds: detection, associations and clinical implications. *Front Neurol Neurosci* 37:78–92
17. Poels MM, Ikram MA, Vernooij MW (2012) Improved MR imaging detection of cerebral microbleeds more accurately identifies persons with vasculopathy. *AJNR Am J Neuroradiol* 33:1553–1556
18. Charidimou A, Wilson D, Shakeshaft C, Ambler G, White M, Cohen H, Yousry T, Al-Shahi Salman R, Lip G, Houlden H, Jäger HR, Brown MM, Werring DJ (2015) The Clinical Relevance of Microbleeds in Stroke study (CROMIS-2): rationale, design, and methods. *Int J Stroke* 10(Suppl A100):155–161
19. Ungvari Z, Tarantini S, Kirkpatrick AC, Csiszar A, Prodan CI (2017) Cerebral microhemorrhages: mechanisms, consequences, and prevention. *Am J Physiol Heart Circ Physiol* 312:H1128–H1143
20. Cordonnier C, Potter GM, Jackson CA, Doubal F, Keir S, Sudlow CL, Wardlaw JM, Al-Shahi Salman R (2009) Improving interrater agreement about brain microbleeds: development of the Brain Observer MicroBleed Scale (BOMBS). *Stroke* 40:94–99
21. van Veluw SJ, Charidimou A, van der Kouwe AJ, Lauer A, Reijmer YD, Costantino I, Gurol ME, Biessels GJ, Frosch MP, Viswanathan A, Greenberg SM (2016) Microbleed and microinfarct detection in amyloid angiopathy: a high-resolution MRI-histopathology study. *Brain* 139:3151–3162
22. Sepehry AA, Lang D, Hsiung GY, Rauscher A (2016) Prevalence of brain microbleeds in Alzheimer disease: a systematic review and meta-analysis on the influence of neuroimaging techniques. *AJNR Am J Neuroradiol* 37:215–222
23. Poliakova T, Levin O, Arablinskiy A, Vasenina E, Zerr I (2016) Cerebral microbleeds in early Alzheimer's disease. *J Neurol* 263:1961–1968
24. Chawla YK, Kashinath RC, Duseja A, Dhiman RK (2011) Predicting mortality across a broad spectrum of liver disease—an assessment of model for End-Stage Liver Disease (MELD), Child–Turcotte–Pugh (CTP) and creatinine-modified CTP scores. *J Clin Exp Hepatol* 1:161–168
25. Wilson D, Jäger HR, Werring DJ (2015) Anticoagulation for atrial fibrillation in patients with cerebral microbleeds. *Curr Atheroscler Rep* 17:47
26. Charidimou A, Kakar P, Fox Z, Werring DJ (2013) Cerebral microbleeds and recurrent stroke risk: systematic review and meta-analysis of prospective ischemic stroke and transient ischemic attack cohorts. *Stroke* 44:995–1001
27. Ueno H, Naka H, Ohshita T, Kondo K, Nomura E, Ohtsuki T, Kohriyama T, Wakabayashi S, Matsumoto M (2008) Association between cerebral microbleeds on T2*-weighted MR images and recurrent hemorrhagic stroke in patients treated with warfarin following ischemic stroke. *AJNR Am J Neuroradiol* 29:1483–1486
28. The Criteria Committee of the New York Heart Association (1994) Nomenclature and criteria for diagnosis of diseases of the heart and great vessels, 9th edn. Mass: Little, Brown & Co, Boston, pp 253–256
29. Gregoire SM, Chaudhary UJ, Brown MM, Yousry TA, Kallis C, Jäger HR, Werring DJ (2009) The Microbleed Anatomical Rating Scale (MARS): reliability of a tool to map brain microbleeds. *Neurology* 73:1759–1766
30. Wu Z, Mittal S, Kish K, Yu Y, Hu J, Haacke EM (2009) Identification of calcification with MRI using susceptibility-weighted imaging: a case study. *J Magn Reson Imaging* 29:177–182
31. Lau WL, Huisa BN, Fisher M (2017) The cerebrovascular-chronic kidney disease connection: perspectives and mechanisms. *Transl Stroke Res* 8:67–76
32. Kim SH, Shin DW, Yun JM, Lee JE, Lim JS, Cho BL, Kwon HM, Park JH (2017) Kidney dysfunction and cerebral microbleeds in neurologically healthy adults. *PLoS One* 12:e0172210
33. Ovbiagele B, Wing JJ, Menon RS, Burgess RE, Gibbons MC, Sobotka I, German L, Shara NM, Fernandez S, Jayam-Trouth A, Edwards DF, Kidwell CS (2013) Association of chronic kidney disease with cerebral microbleeds in patients with primary intracerebral hemorrhage. *Stroke* 44:2409–2413

34. Watanabe A (2007) Cerebral microbleeds and intracerebral hemorrhages in patients on maintenance hemodialysis. *J Stroke Cerebrovasc Dis* 16:30–33
35. Li L, Fisher M, Lau WL, Moradi H, Cheung A, Thai G, Handwerker J, Kalantar-Zadeh K (2015) Cerebral microbleeds and cognitive decline in a hemodialysis patient: case report and review of literature. *Hemodial Int* 19:E1–E7
36. Song TJ, Kim J, Lee HS, Nam CM, Nam HS, Kim YD, Heo JH (2014) Distribution of cerebral microbleeds determines their association with impaired kidney function. *J Clin Neurol* 10:222–228
37. Haley KE, Greenberg SM, Gurol ME (2013) Cerebral microbleeds and macrobleeds: should they influence our recommendations for antithrombotic therapies? *Curr Cardiol Rep* 15:425
38. Lee SH, Ryu WS, Roh JK (2009) Cerebral microbleeds are a risk factor for warfarin-related intracerebral hemorrhage. *Neurology* 72:171–176
39. Teperman LW (2013) Impact of pretransplant hepatic encephalopathy on liver posttransplantation outcomes. *Int J Hepatol*. 2013:952828
40. Rovira A, Alonso J, Córdoba J (2008) MR imaging findings in hepatic encephalopathy. *AJNR Am J Neuroradiol* 29:1612–1621
41. Kim YD, Song D, Heo JH, Kim SU, Kim BK, Park JY, Kim DY, Ahn SH, Kim KJ, Han KH (2015) Relationship between cerebral microbleeds and liver stiffness determined by transient elastography. *PLoS One* 10:e0139227
42. Achiriloaie AF, Kido D, Wycliffe D, Jacobson JP (2011) White matter microsusceptibility changes in patients with hepatic encephalopathy. *J Radiol Case Rep* 5:1–7